Available online at www.sciencedirect.com

ScienceDirect

journal homepage: www.elsevier.com/locate/he

Evaluation of an iron-chlorine thermochemical cycle for hydrogen production

CrossMark

Cristian Canavesio, Horacio E. Nassini, Ana E. Bohé[*]

Complejo Tecnológico Pilcaniyeu, Comisión Nacional de Energía Atómica, Avenida Bustillo 9500, 8400 San Carlos de Bariloche, Argentina

ABSTRACT

In this paper, a theoretical and experimental study on an iron-chlorine thermochemical cycle for hydrogen production is presented. The study was addressed to confirm the occurrence of the thermochemical reactions originally proposed and to investigate the influence of kinetic parameters for improving the overall performance of this cycle. Firstly, a thermodynamic analysis was done for determining whether this cycle is attractive for hydrogen production at reaction temperatures below 1223 K, in terms of both energy efficiency and yield of hydrogen. Following, proof-of-concept experiments using a batch reactor were performed at different reaction temperatures, pressures and holding times. Experimental results showed that the reaction temperature is expected to have a small effect for increasing the hydrogen production, while an increase of the system pressure was observed to raise markedly the conversion degree achieved. Based on experimental results, it was possible to confirm the reaction pathway of thermochemical reactions originally proposed, to identify the rate determining step of the overall process, and to explain the beneficial effect of increasing the system pressure on the hydrogen yield. Finally, a modified cycle is proposed for increasing its overall energy efficiency, by lowering the reaction temperature of two thermochemical reactions from 1198 K to 923 K in order to avoid the phase change of $FeCl_2$ that melts at 950 K. Comparative calculations of enthalpy balance and external heat and work requirements for the original and modified cycles showed that the limiting energy efficiency could be theoretically increased from the range 24—28% to 32—37% and this significant increment appears to be promising for further investigations.

Copyright © 2015, Hydrogen Energy Publications, LLC. Published by Elsevier Ltd. All rights reserved.

Introduction

The expansion of the world's population and economy resulted in a twenty fold rise in the use of fossil fuels during the 20th century and it is expected that the current level would be doubled by 2050. Neither the trend nor the degree of the current dependence on fossil fuels is considered sustainable since the resources of oil, gas, and coal are known to be finite and because the intensive use produces serious climatic effects. Alternative fuels are then needed on a scale that can keep humanity's development continual in this century and

beyond, while avoiding or minimizing the undesirable greenhouse gas emissions to the atmosphere.

Hydrogen is such an alternative fuel since it is clean burning, has a large capacity as a carrier of energy, and can be generated from many sources using different processes like natural gas reforming, coal gasification, water electrolysis, and thermochemical water-splitting cycles. Development of suitable technologies for the efficient production and storage of hydrogen represents the most important technical challenges for realizing the hydrogen energy system in the near future [1—3].

The concept of thermochemical water-splitting cycles offers an attractive candidate for the large-scale production of hydrogen. Direct thermal decomposition of water molecule requires high temperature heat of exceeding 2273 K but thermochemical water-splitting processes make it possible to decompose water at lower temperatures by combining high-temperature endothermic chemical reactions and low-temperature exothermic ones within a closed loop, where only heat and water are supplied and all reactants are recycled internally [4].

Research activities on thermochemical water-splitting cycles were started by Funk and Reinstrom during sixties [5]. Since then, many active studies have been carried out in several countries and a number of different cycles have been proposed [6]. Even though more than 200 thermochemical cycles have been identified for the water splitting, very few of them have progressed beyond theoretical calculations to experimental demonstrations, based on performance requirements like high thermal efficiency of hydrogen production, good matching with the high-temperature heat sources, easy plant operation, and easy scaling up of experimental facilities. The iodine-sulphur (I—S) cycle is the most famous and well-studied version of these cycles which was proposed by General Atomics [7], and it is one of the most promising processes regarding the utilization of nuclear heat sources which can supply heat at temperatures close to 1273 K [8].

Majority of thermochemical water-splitting cycles that are being proposed, like the I—S cycle, requires heat supply at temperatures above 1073 K. Based on benefits arising from the use of lower process temperatures, i.e. cost reduction of materials and maintenance, use of low-grade waste heat, that effectively improve the cycle and power plant efficiencies, several alternative cycles based on metallic chlorides are being investigated with the goal of reducing the process temperatures to the order of 773—973 K. In the framework of the Nuclear Hydrogen Initiative [9], four metallic chloride-based thermochemical water-splitting cycles have been identified after considering factors like thermal efficiency, cost analysis and feasibility of industrialization: (1) copper-chlorine (Cu-Cl) [10]; (2) cerium-chlorine (Ce-Cl) [11]; iron-chlorine (Fe-Cl) [12]; and vanadium-chlorine (V-Cl) [13]. All of them decompose the water molecule into hydrogen and oxygen through several reaction steps that involve metal and chlorine compounds.

In this paper, a theoretical and experimental study on a Fe-Cl thermochemical cycle for hydrogen production is presented. This cycle was selected after considering factors such as availability and abundance of reagent materials, simplicity, chemical viability and thermodynamic feasibility, and the study was addressed to elucidate the reaction pathway and the kinetics of the overall cycle with the objective of improving its efficiency in terms of both energy and hydrogen yield, as a previous step for a further scaling up of experimental facilities.

The iron-chlorine family of cyles

The Fe-Cl family of cycles has been considered potentially attractive for hydrogen production and investigations were carried out in Germany, Japan, U.S.A. and Italy [12,14—17]. The major attraction of cycles of this family is the fact that the chemicals involved are common and relatively cheap.

The Fe-Cl family of cycles was proposed in the early of 1970 at the Aachen University, Germany, and one example of these cycles is the so-called Mark-15 cycle [18] that was selected for the present evaluation. The Mark-15 cycle, which is schematically shown in Fig. 1, involves the following four chemical reaction steps for the water splitting process [19]:

$$3FeCl_2(l) + 4H_2O(g) \rightarrow Fe_3O_4(s) + 6HCl(g) + H_2(g) \quad T = 1198 \text{ K}, \quad \Delta H = +156.1 \text{ kJ} \tag{1}$$

$$Fe_3O_4(s) + 8HCl(g) \rightarrow FeCl_2(s) + 2FeCl_3(s) + 4H_2O(g) \quad T = 398 \text{ K}, \quad \Delta H = -244.5 \text{ kJ} \tag{2}$$

$$2FeCl_3(g) \rightarrow 2FeCl_2(s) + Cl_2(g) \quad T = 698 \text{ K}, \Delta H = -160.5 \text{ kJ} \tag{3}$$

$$Cl_2(g) + H_2O(g) \rightarrow 2HCl(g) + \tfrac{1}{2}O_2(g) \quad T = 1198 \text{ K}, \Delta H = +59.4 \text{ kJ} \tag{4}$$
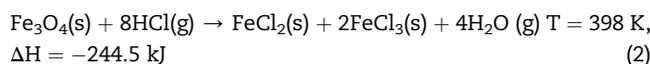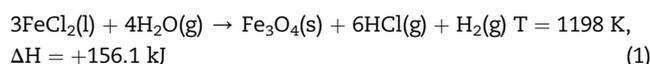
Then, the global water-splitting reaction is:

$$H_2O \rightarrow H_2 + \tfrac{1}{2}O_2 \tag{5}$$

Even though the temperatures for two of the reactions exceed 1173 K, experimental work showed that the two high-temperature reactions could be run at lower temperatures in the range between 798 K and 1198 K [20].

Many attempts were made to solve the technological problems associated with this cycle, but no suitable solution was found up to now because the kinetics and fundamental mechanisms of thermochemical reactions are not completely understood yet.

Thermodynamic analysis

First of all, a complete thermodynamic analysis was carried out in order to determine whether the Mark-15 Fe-Cl cycle may be attractive for hydrogen production in terms of both energy efficiency and yield of desired products, at process temperatures lower than 1223 K. The HSC software was used for the thermodynamic calculations presented below [21].
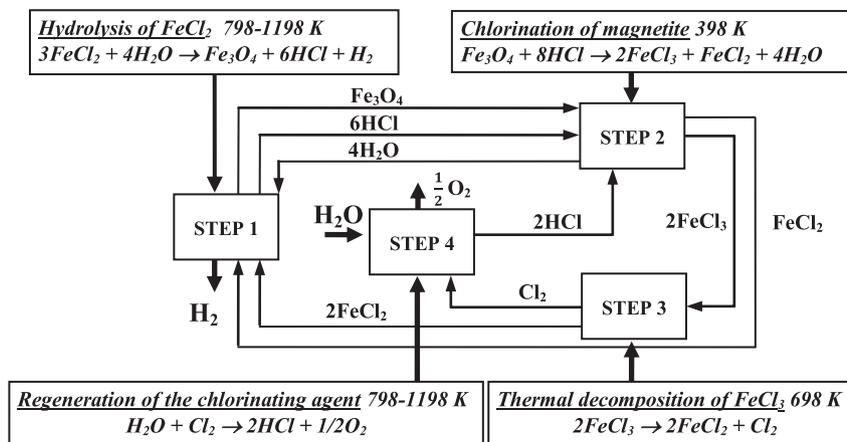
Fig. 1 – Mark-15 Fe-Cl thermochemical cycle for water splitting.

Evaluation of the limiting energy efficiency

The limiting energy efficiency expected for the Mark-15 Fe-Cl cycle was firstly estimated according to the methodology described in Ref. [22]. Calculation of limiting energy efficiency assumes an idealized process in which the thermochemical water-splitting reactions given by Equations (1)–(4) are considered to be fully completed. Heat and work inputs to the process at the reaction temperatures were estimated as follows: heat inputs were based on the enthalpy and heat capacity data for sensible and latent heats of different species which were obtained from the HSC database, while the external heat demand could be calculated by using pinch analysis [23]; work inputs comprise the separation work of the product streams and the chemical potential work.

The definition of energy efficiency, ξ, given in Ref. [18] was used as a measure of the cycle performance for initial screening purposes and it is equal to the ratio between the energy output of the process and the total energy put into the system:

$$\xi = \frac{-\Delta H^o_{(H_2O)}}{Q_{process} + W_T/0,5} \tag{6}$$

In this equation, $\Delta H^o_{(H2O)}$ is the standard enthalpy of the formation of: (a) liquid water at 298 K, 285.8 kJ/mol,; or (b) water vapor at 298 K and atmospheric pressure, 241.8 kJ/mol. The first value corresponds to the higher heating value of hydrogen (HHV) and the second one to the lower heating value of hydrogen (LHV). $Q_{process}$ is the heat supplied to the process from external sources while $W_T/0.5$ represents the thermal equivalent of different types of work put into the process and assuming 50% efficiency for the conversion of heat into work. This conversion efficiency is that expected in the case of using high temperature gas cooled nuclear reactors as heat process sources.

The evaluation of the limiting energy efficiency of the Mark-15 Fe-Cl cycle was normalized to 1 mol of product hydrogen. The liquid water was assumed to enter the thermochemical process at 298 K and both hydrogen and oxygen were considered to leave the process at 298 K and atmospheric pressure. For the enthalpy balance of thermochemical

reactions given by Equations (1)–(4), the Mark-15 Fe-Cl cycle was firstly decomposed in a series of elementary steps as shown in Fig. 2. Following, the enthalpy change for each elementary step was calculated and an overall thermal energy balance was performed for the closed cycle. Physical and chemical properties of different species involved in reactions were obtained from the HSC database.

In Table 1, the individual steps representing the operation of the Mark-15 Fe-Cl cycle are summarized. T_{in} and T_{out} correspond to the starting and finishing temperatures of each individual step while ΔH y ΔG represent the changes of enthalpy and standard Gibbs free energy, respectively. The first four steps detailed in Table 1 comprise the thermochemical reactions given by Equations (1)–(4), while the remaining eighteen steps involve the heating and cooling processes up to reach the reaction temperatures, as well as the phase changes of different products and reactants such as H_2O, $FeCl_2$ and $FeCl_3$.

Furthermore, for the thermal energy balance and recovery within the thermochemical process, a pinch analysis was applied to estimate the maximum amount of heat that can be recovered and recycled internally, matching the various hot and cold process streams on the basis of the available heat loads and a minimum practical temperature difference driving force of 10 K.

On the other hand, the ideal work of separation was calculated by the following equation [24]:

$$\Delta G_{sep} = -R \cdot T \cdot \sum_i n_i \cdot \ln(y_i), \tag{7}$$

where ΔG_{sep} is the Gibbs energy of mixing or the minimum energy required for the separation of the product streams, R is the universal gas constant, T is the absolute temperature, and n_i and y_i are the number of moles and the molar fraction of the product "i", respectively.

Finally, the chemical potential work required by a reaction was defined as the positive free energy change of the reaction, and considering that no credit is taken for this theoretically recoverable energy when the free energy change is negative.

Table 2 shows the different components of the thermal energy required for producing 1 mol of hydrogen through the
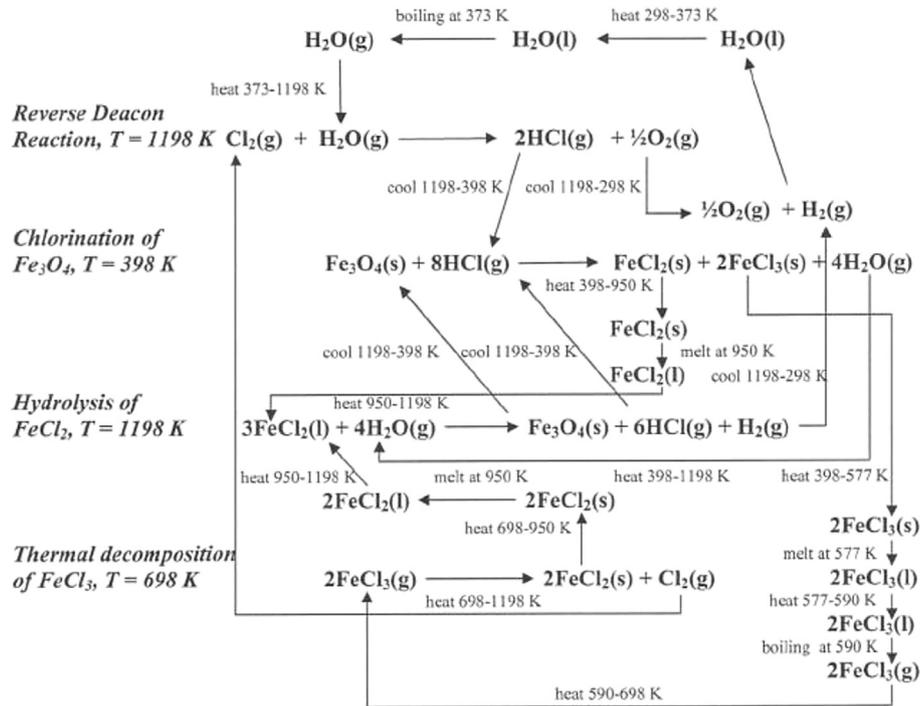
Fig. 2 – Decomposition of the Mark-15 Fe-Cl cycle into elementary steps for thermal enthalpy balance analysis.

Mark-15 Fe-Cl cycle. Calculation of the heat equivalent from work inputs assumes a 50% conversion factor which is based on the heat available from a high-temperature gas cooled nuclear reactor.

By applying Equation (6), the limiting energy efficiencies of the Mark-15 Fe-Cl cycle are expected to be:

- Lower heating value of hydrogen (LHV): $\xi = \frac{241.8}{1014.9} \times 100 = 24\%$
- Higher heating value of hydrogen (HHV): $\xi = \frac{285.8}{1014.9} \times 100 = 28\%$

It is noted that these energy efficiency values calculated for the Mark-15 cycle are consistent with the estimation given in

Table 1 – Enthalpy balance for the Mark-15 Fe-Cl cycle.

Compound	Reaction	Type	Moles	Tin [K]	Tout [K]	ΔH [kJ]	ΔG [kJ]
$Fe_3O_4(s)$	$Fe_3O_4 + 8HCl \rightarrow FeCl_2 + 2FeCl_3 + 4H_2O$	Reaction	1	398	398	−244.5	−58.9
$FeCl_2(l)$	$3FeCl_2 + 4H_2O \rightarrow Fe_3O_4 + 6HCl + H_2$	Reaction	3	1198	1198	156.1	222.7
$FeCl_3(g)$	$2FeCl_3 \rightarrow 2FeCl_2 + Cl_2$	Reaction	2	698	698	−160.5	−23.9
$Cl_2(g)$	$Cl_2 + H_2O \rightarrow 2HCl + ½O_2$	Reaction	1	1198	1198	59.4	−22.5
$H_2O(l)$	Sensible	Heat 298-373 K	1	298	373	5.7	
$H_2O(l) \rightarrow H_2O(g)$	Latent	Boiling	1	373	373	40.9	
$H_2O(g)$	Sensible	Heat 373-1198 K	1	373	1198	29.7	
$H_2O(g)$	Sensible	Heat 398-1198 K	4	398	1198	115.2	
$Cl_2(g)$	Sensible	Heat 698-1198 K	1	698	1198	12.0	
$FeCl_3(s)$	Sensible	Heat 398-577 K	2	398	577	47.3	
$FeCl_3(s) \rightarrow FeCl_3(l)$	Latent	Melting	2	577	577	112.9	
$FeCl_3(l)$	Sensible	Heat 577-590 K	2	577	590	3.4	
$FeCl_3(l) \rightarrow FeCl_3(g)$	Latent	Boiling	2	590	590	154.0	
$FeCl_3(g)$	Sensible	Heat 590-698 K	2	590	698	28.1	
$FeCl_2(s)$	Sensible	Heat 398-698 K	1	398	698	27.0	
$FeCl_2(s)$	Sensible	Heat 698-950 K	3	698	950	68.0	
$FeCl_2(s) \rightarrow FeCl_2(l)$	Latent	Melting	3	950	950	41.1	
$FeCl_2(l)$	Sensible	Heat 950-1198 K	3	950	1198	75.9	
$Fe_3O_4(s)$	Sensible	Cool 1198-398 K	1	1198	398	−114.4	
$HCl(g)$	Sensible	Cool 1198-398 K	8	1198	398	−192.0	
$O_2(g)$	Sensible	Cool 1198-298 K	0.5	1198	298	−14.4	
$H_2(g)$	Sensible	Cool 1198-298 K	1	1198	298	−26.1	
					TOTAL	224.8	

Table 2 – Heat and work inputs estimated for the Mark-15 Fe-Cl cycle.		
	Energy [kJ/mol H_2]	Heat equivalent[a] [kJ/mol H_2]
Heat-in	224.8	224.8
Heat rejected	205.7	205.7
Separation work	69.5	139.0
Chemical potential work	222.7	445.4
Sum of heat and work inputs		1014.9

[a] A 50% conversion factor is assumed which is based on the heat available from a high-temperature gas cooled nuclear reactor.

Refs. [19], 29% (LHV), while they are quite below of 43% that was reported formerly by Carty et al. in Ref. [25].

Calculation of equilibrium compositions

In a second step of the thermodynamic analysis, the equilibrium amounts of the different species were evaluated for several conditions of temperature and pressure.

Analysis was initiated with non-stoichiometric amounts of $FeCl_2$ and H_2O as given by Equation (1). For a H_2O:$FeCl_2$ ratio equal to 1:1 in moles, the equilibrium composition in the gaseous phase shows that the amount of H_2 increases with temperature from 3.71×10^{-2} mol at 823 K to 1.41×10^{-1} mol at 1223 K, as it is seen in Table 3. Considering that the initial amount of water was 1 mol, the calculated values indicate that the cycle has reached the equilibrium, producing a conversion percentage of 3.7% at 823 and 14.1% at 1223 K, respectively. Other species in the gaseous phase are mostly un-reacted H_2O and un-dissociated HCl, while $FeCl_2$, $FeCl_3$, Cl_2, and O_2 are expected to be also present as impurities. In the condensed phase, only $FeCl_2$ is predicted to have a minimum reaction while a small amount of Fe_3O_4 is believed to be also formed, but any Fe_2O_3 is expected to be present in equilibrium.

If a greater amount of water is added to the system, increasing the ratio H_2O:$FeCl_2$ from 1:1 to 4:2 in moles, it is observed a slight change in the relative amounts of different species at all temperatures, as shown in Table 4. Changes with temperature of H_2O, H_2, HCl, $FeCl_2$, $FeCl_3$ and Cl_2 are less pronounced than in the previous case. For example, they are from 85 mol% to 59 mol% for H_2O (instead 85 mol% to 44 mol%) at 823 K and 1223 K, respectively, while the relative change of O_2 increases from 4.89×10^{-23} mol% to 7.61×10^{-14} mol% compared with 1.22×10^{-23} mol% to 7.56×10^{-15} mol% for the previous case. It is expected that the percentage of water increases and the percentage of the other species decreases. Nevertheless, the final equilibrium amount of O_2 at 1223 K is

greater than before. In the condensed phase, it is observed a less amount of $FeCl_2$ and a greater amount of Fe_3O_4 at all temperatures.

These calculation results indicate that the presence of water in excess creates an oxidative atmosphere which is not convenient for the formation of hydrogen. Therefore, it is expected that the dissociative reaction of HCl would be inhibited by the presence of more amounts of water in reactions given by Equations (2) and (4).

On the other hand, if the amount of $FeCl_2$ is increased, there is no change in the fraction of the gaseous phase. Calculations were done with H_2O:$FeCl_2$ ratio equal to 1:4 in moles and results were similar to those given in Table 3. This result means that the condensed chloride does not affect the equilibrium amount without beneficiating the hydrogen reaction.

If the system pressure is increased, no significant changes in the equilibrium calculations are observed to occur for all temperatures tested. The increase of the system pressure is expected to produce a small increment in the production of hydrogen with respect to the value reached at atmospheric pressure. The equilibrium amounts of gaseous species for a system pressure of 3 atm and ratios H_2O:$FeCl_2$ of 1:1 and 4:2 in moles are presented in Tables 5 and 6, respectively.

According to thermodynamic calculation results, the most convenient conditions for increasing the hydrogen production through the Mark-15 Fe-Cl cycle correspond to a water supply in amounts below the stoichiometric value given by Equation (1) at normal pressure, and using reaction temperatures as high as possible above 923 K. In the following, details of the experimental setup used for the proof-of-concept tests with the premise of maintaining the water reactant in defect are presented.

Proof-of-concept experiments

Materials

The solid reactant used for producing the Mark-15 cycle thermochemical reactions was a green powder of tetra-hydrated iron chloride ($FeCl_2 \cdot 4H_2O$) manufactured by Alfa Aesar Company. The gas used as carrier gas for chromatography determinations and for providing an inert atmosphere into the reactor was argon 99.99% purity (AGA, Argentina).

Experimental setup and test procedure

Thermochemical reactions were produced starting with vacuum conditions using a quartz reactor that is schematically shown in Fig. 3. The reactor is located inside an electrical

Table 3 – Equilibrium calculation of gaseous phase composition at atmospheric pressure (H_2O:$FeCl_2$ ratio equal to 1:1 in moles).							
Temperature [K]	H_2O (g) [mol]	HCl (g) [mol]	$FeCl_2$ (g) [mol]	H_2 (g) [mol/(% conversion)]	$FeCl_3$ (g) [mol]	Cl_2 (g) [mol]	O_2 (g) [mol]
823	8.52×10^{-01}	2.23×10^{-01}	3.00×10^{-04}	3.71×10^{-02} (3.7%)	5.82×10^{-07}	3.00×10^{-13}	1.22×10^{-23}
923	7.03×10^{-01}	4.45×10^{-01}	6.67×10^{-03}	7.42×10^{-02} (7.4%)	1.29×10^{-05}	1.18×10^{-11}	5.70×10^{-21}
1223	4.36×10^{-01}	8.45×10^{-01}	5.76×10^{-01}	1.41×10^{-01} (14.1%)	6.58×10^{-04}	9.33×10^{-09}	7.56×10^{-15}

Table 4 – Equilibrium calculation of gaseous phase composition at atmospheric pressure (H_2O:$FeCl_2$ ratio equal to 4:2 in moles).

Temperature [K]	H_2O (g) [mol]	HCl (g) [mol]	$FeCl_2$ (g) [mol]	H_2 (g) [mol/(% conversion)]	$FeCl_3$ (g) [mol]	Cl_2 (g) [mol]	O_2 (g) [mol]
823	3.41	8.90×10^{-01}	1.20×10^{-03}	1.48×10^{-01} (3.7%)	2.33×10^{-06}	1.20×10^{-12}	4.89×10^{-23}
923	2.81	1.78	2.67×10^{-02}	2.97×10^{-01} (7.4%)	5.14×10^{-05}	4.71×10^{-11}	2.28×10^{-20}
1223	2.34	2.48	7.57×10^{-01}	4.15×10^{-01} (11%)	8.56×10^{-04}	2.75×10^{-08}	7.61×10^{-14}

Table 5 – Equilibrium calculation of gaseous phase composition at 3 atm (H_2O:$FeCl_2$ ratio equal to 1:1 in moles).

Temperature [K]	H_2O (g) [mol]	HCl (g) [mol]	$FeCl_2$ (g) [mol]	H_2 (g) [mol/(% conversion)]	$FeCl_3$ (g) [mol]	Cl_2 (g) [mol]	O_2 (g) [mol]
823	9.06×10^{-01}	1.42×10^{-01}	9.63×10^{-05}	2.36×10^{-02} (2.4%)	2.63×10^{-07}	1.91×10^{-13}	1.1×10^{-23}
923	8.05×10^{-01}	2.92×10^{-01}	2.08×10^{-03}	4.87×10^{-02} (4.8%)	5.81×10^{-06}	7.72×10^{-12}	5.42×10^{-21}
1223	5.16×10^{-01}	7.25×10^{-01}	3.21×10^{-01}	1.21×10^{-01} (12.1%)	6.41×10^{-04}	8.0×10^{-09}	4.05×10^{-15}

Table 6 – Equilibrium calculation of gaseous phase composition at 3 atm (H_2O:$FeCl_2$ ratio equal to 4:2 in moles).

Temperature [K]	H_2O (g) [mol]	HCl (g) [mol]	$FeCl_2$ (g) [mol]	H_2 (g) [mol/(% conversion)]	$FeCl_3$ (g) [mol]	Cl_2 (g) [mol]	O_2 (g) [mol]
823	3.62	5.67×10^{-01}	3.85×10^{-04}	9.44×10^{-02} (2.7%)	1.05×10^{-06}	7.64×10^{-13}	4.39×10^{-23}
923	3.22	1.17	8.31×10^{-03}	1.95×10^{-01} (4.9%)	2.32×10^{-05}	3.09×10^{-11}	2.17×10^{-20}
1223	2.34	2.48	7.56×10^{-01}	4.14×10^{-01} (10.4%)	1.48×10^{-03}	2.74×10^{-08}	2.54×10^{-14}
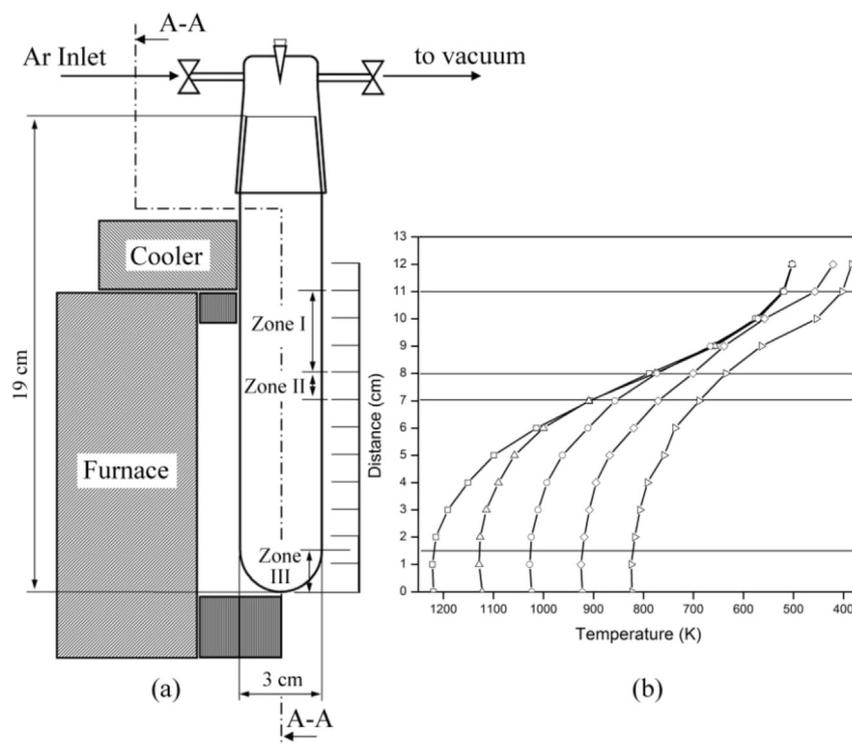
Fig. 3 – (a) Quartz reactor used for the Mark-15 proof-of-concept experiments. (b) Axial temperature profiles for different setup temperatures.

tubular furnace with a temperature gradient and experiments were carried out at temperatures at the bottom of the reactor in the range between 823 K and 1223 K during different reaction times, ranging from 1 h to 72 h.

In all proof-of-concept tests, a weighed amount of $FeCl_2 \cdot 4H_2O$ (green powder) was located in the bottom zone of the reactor (Zone III). The reactor was then purged with a vacuum pump for two hours up to reach a system pressure of 1.0×10^{-4} bar; during this degassing step the solid reactant is expected to lose two molecules of water staying in the reactor as $FeCl_2 \cdot 2H_2O$, which was verified by X-Ray diffraction (XRD). Afterwards, the reactor was heated from room temperature to the reaction temperature selected for the test. Around the neck of the reactor (6 cm from the top of the reactor body), cooling water was continuously supplied through a serpentine cooler in order to avoid the sticking of the lubricant-sealant between the reactor body and lid.

When the reaction time selected for the test was consumed, the reactor was retired from the electrical furnace and left to cool to room temperature. After reactor disassembling, visual inspections were made and different condensed products were detected, as a function of the axial temperature profile produced along the reactor body. Solid products were separated in inert atmosphere on the basis of their morphologies and colors, and all of them were characterized by XRD and scanning electron microscopy (SEM 515, Philips Electronics Instruments).

Furthermore, the gaseous phase in the reactor was analyzed in two stages. Firstly, 100 μl of gaseous products were removed from the reactor at room temperature through a septum and bubbled into a $AgNO_3$ solution in order to detect the presence of HCl(g). Secondly, the reactor was immersed in a bath of liquid nitrogen to condense all gaseous species with the exception of hydrogen. With this experimental procedure, the corrosive species were condensed and the hydrogen produced could be analyzed by gas chromatography without affecting the thermal conductivity detector (TCD) and the flame ionization detector (FID).

The hydrogen content in the gaseous phase was determined by using a SRI 8610C gas chromatographer equipped with Alltech® CTR concentric packed columns, which consists essentially in a column within a column that allows use two different packing for the analysis of the sample. The outer column is 6 ft × 1/4″ packed with activated molecular sieve and the inner column is 6 ft × 1/8″ packed with porous polymer mixture. The working conditions of the gas chromatographer were: pressure = 0.83 bar; furnace temperature = 315 K; flow rate of the carrier gas (argon 99.99% purity) = 30 ml/min; temperature of TCD = 373 K; current = 125 mA.

The gaseous sample was taken from the reactor through a direct connection to the loop, which was previously in vacuum, and then introduced into the chromatographer by switching on the loop. Fig. 4(a) shows a typical chromatogram after an experiment. The amount of each species was calculated by integrating in Fig. 4 the output signal of the TCD and these results are expressed as peak areas. Taking into account the column used, the retention time of hydrogen was, in this case, 52.4 s.

In order to determine the amount of hydrogen produced during thermochemical reactions, it was necessary to accomplish a proper calibration of the system addressed to obtain a relationship between the peak areas obtained with the gaseous sample extracted from the reactor and the amounts of hydrogen produced during reactions.

The following calibration procedure by using pure hydrogen gas (99.995% purity, AGA, Argentina) was carried out: the reactor was firstly purged with a vacuum pump up to 1.0×10^{-4} bar, then 2 ml of pure hydrogen gas was added at time intervals until to reach 38 ml that corresponds to 100% conversion of hydrogen produced from 150 mg of $FeCl_2 \cdot 4H_2O$. After each addition step, the system was left to stabilize and the final hydrogen concentration into the reactor was calculated. Following, a gaseous phase sample of 1 ml was extracted from the reactor through the vacuum loop and injected into the gas chromatographer, measuring the peak area from the corresponding chromatogram. Finally, a calibration curve was constructed representing the relationship between the hydrogen concentration into the reactor (in mmol) and the peak area of the respective chromatogram (in arbitrary units). A good linearity of the calibration curve from a regression analysis was obtained, as shown in Fig. 4(b).

After calibration of the system, it was possible to determine the hydrogen concentration in the reactor after different reaction times, by interpolating in the calibration curve the values of the hydrogen peak areas obtained with samples of
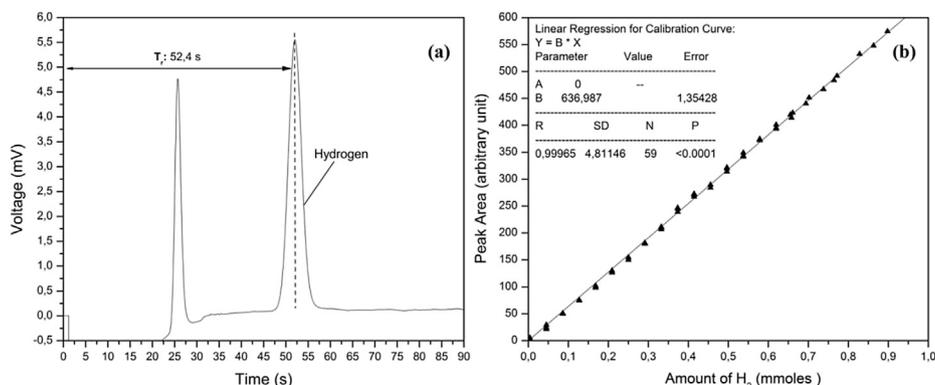
Fig. 4 – : (a) Typical chromatogram obtained after a Fe-Cl cycle experiment. (b) Calibration curve for the hydrogen production determination.
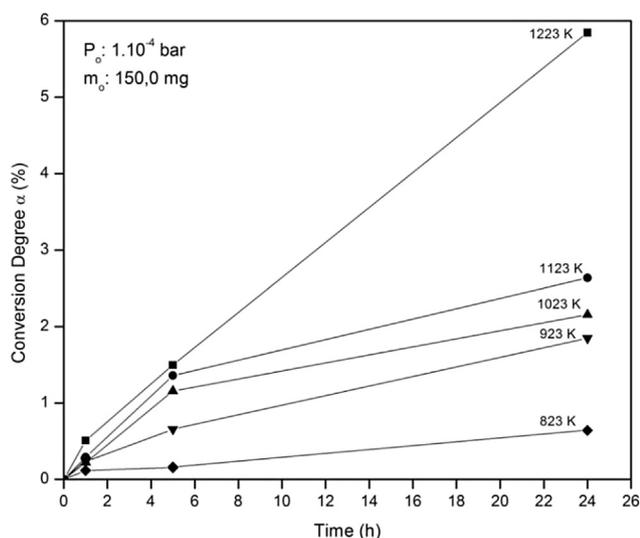
Fig. 5 – Conversion degree as a function of reaction time for different test temperatures.

1 ml sucked from the reactor. The conversion degree was calculated by the following equation:

$$\alpha\% = \frac{Area}{CS} \times \frac{PM_{FeCl_2 \cdot 4H_2O}}{2 * m_{0FeCl_2 \cdot 4H_2O}} \times 100, \tag{8}$$

where: $\alpha\%$ is the conversion degree (in %), $Area$ is the chromatogram peak area, $m_{0FeCl_2 \cdot 4H_2O}$ is the initial mass of the sample (in g), $PM_{FeCl_2 \cdot 4H_2O}$ is the molecular weight of the $FeCl_2.4H_2O$, and CS is the slope of the calibration curve.

Results and discussion

Three experiments were carried out at each temperature selected, following the procedure described previously. Fig. 5 shows typical conversion degree ($\alpha\%$) vs. time (in hours) curves for reaction temperatures ranging from 823 K to 1223 K. As can be seen, after 1 h of heating the conversion degree attained in all cases was below 0.5%, but it was observed a beneficial effect of the reaction temperature on hydrogen production: as expected, when the reaction temperature was increased, the conversion degree increased too. After 24 h of continuous heating, the conversion degree was observed to increase markedly and the temperature effect became more evident: 1.8% conversion at 923 K and above 5.5% conversion at 1223 K.

Table 7 – Reaction rates at different temperatures from 823 K to 1223 K.			
Reaction rate [1/s]	T [K]	ln (R)	1/T [1/K]
0.00006842	1223	−9.589845	0.0008177
0.00003209	1123	−10.34697	0.0008905
0.00002608	1023	−10.55434	0.0009775
0.00002209	923	−10.72039	0.0010834
0.00000757	823	−11.79132	0.0012151

Since all experimental values obtained were lower than the equilibrium amounts estimated by thermodynamic calculations, i.e. $\alpha\% = 3.7\%$ at 823 K, $\alpha\% = 7.4\%$ at 923 K, and $\alpha\% = 14.1\%$ at 1223 K, respectively, it can be concluded that the thermochemical reactions did not achieve the equilibrium conditions for the experimental conditions used in tests. Then, it is possible to estimate the apparent reaction rate by considering the slope of the straight portions of the conversion degree vs. time curves at different temperatures tested. With experimental values obtained at reaction times of 1 h, 5 h and 24 h which are indicated in Fig. 5, the reaction rates were roughly calculated and they are presented in Table 7. It is seen that the overall reaction rate of the Fe-Cl cycle is expected to be very slow.

By using the slope of straight lines depicted in Fig. 5 as if they would represent the reaction rate (v), a plot of ln(v) vs 1/T could be obtained for calculating the apparent activation energy of the process, resulting values in the order of 40 kJ/mol. So this calculated value indicates a very low activation process which reaction rate would be very slightly modified by temperature.

After completion of the experiments, different solid products were observed to be deposited on the inner surfaces of the three reactor zones, and they could be clearly identified by visual inspection. The morphology and color of these solid residues were independent of the reaction temperature and of the amount of hydrogen produced.

In the lid of the reactor (Zone I), a yellowish deliquescent residue was always detected; the amount of this residue and the intensity of its color increase with the amount of initial reagent ($FeCl_2 \cdot 4H_2O$). Taking into account the criteria of the CRC Handbook description [26], it is concluded that this gelatinous substance was $FeCl_3 \cdot xH_2O$ because the ferric chloride is yellowish and deliquescent, so it is difficult to detect by XRD.

Immediately below the Zone I of reactor, which is far away from the reaction zone, a solid white condensed residue on the reactor walls was found. The white crystals were identified by XRD patterns as $FeCl_2 \cdot 2H_2O$ and $FeCl_2 \cdot 4H_2O$, as can be seen in Fig. 6(a). They presented a uniform morphology of platelets as shown in the SEM micrographs of Fig. 7(a–b).

Finally, a fine dark reddish powder was found in the Zones II and III of reactor. Fig. 6(b) shows the XRD pattern of this solid residue and it can be observed that it is in good agreement with the corresponding reference pattern of Fe_3O_4, while a remnant of $FeCl_2 \cdot 2H_2O$ was also detected. The presence of this type of partially reduced iron oxide can be explained by the existence of a low amount of oxygen (about 15 ppb as calculated for the equilibrium conditions for a system pressure of 1.0×10^{-15} bar). This concentration of oxygen is not enough for generating the oxidizing atmosphere required to produce Fe_2O_3.

After analyzing the solid residues produced in the reaction zone of reactor in all experiments, it can be concluded that the only new solid phase produced during thermochemical reactions was the formation of Fe_3O_4 with a well-defined crystal growth, showing its characteristic square bi-pyramidal geometry due to the octahedral typical form, as can be seen in the SEM micrographs of Fig. 7(c–d). Also, the reactor walls were covered by small crystals of this chloride which are the
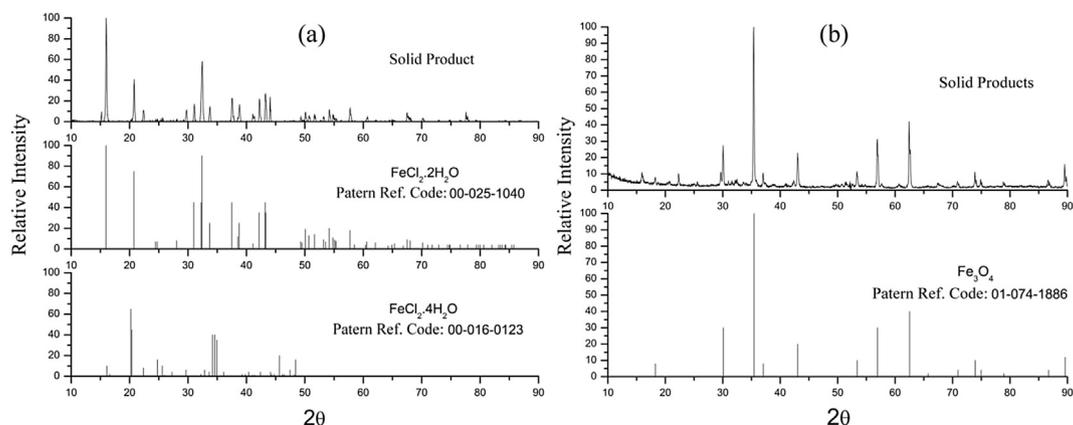
Fig. 6 − : (a) XRD pattern of the solid residue obtained from the Zone I of reactor. (b) XRD pattern of solid residue obtained from the Zones II and III of reactor. T: 823 K, P_o: 1×10^{-4} bar, t: 24 h.

remnant iron chloride (II), forming hexagonal plates of about 100 μm wide, Fig. 7(a–b).

Additional tests were carried out in successive heating steps at the same reaction temperature, extracting the gaseous products from the reactor at each heating step with the procedure described before. The objective of these interrupted tests was to explore whether the extraction of reaction products shifts the thermochemical reactions in a direction that enhances the hydrogen production.

In these interrupted tests, the heating of reactor was shut off after a programmed time and the presence of HCl was detected by the $AgNO_3$ solution proof. Following, the reactor was cooled by immersion in a bath of liquid nitrogen to detect

the presence of hydrogen by gas chromatography. Then, the reactor heating was re-initiated up to reach the reaction temperature and this procedure was repeated three or four times.

For a reaction temperature of 823 K, a reaction degree of 0.14% had been achieved after 1 h of continuous heating. After removing the gaseous products from the reactor, the conversion degree reached during the second heating step was 0.3% while, after five successive heating steps, a final conversion degree of 0.9% could be obtained. As can be observed in Fig. 8, this conversion degree is practically five times greater than the value obtained by the conventional method of heating the reactor during 5 h without removing the gaseous products (α % = 0.16%). From these experimental results, it can be
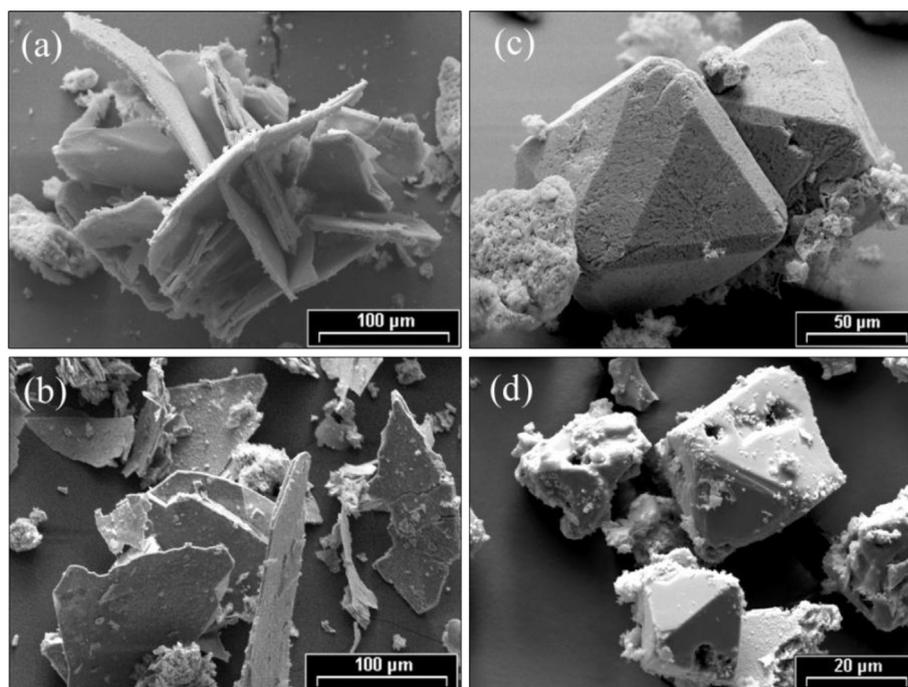
Fig. 7 − SEM micrographs of the solid residues extracted from different zones of reactor: (a–b) from the Zone I; (c–d) from the Zones II and III. Fig. 7(a–c): T: 823 K, P_o: 1×10^{-4} bar, t: 24 h Fig. 7(b–d): T: 1223 K, P_o: 1×10^{-4} bar, t: 24 h.
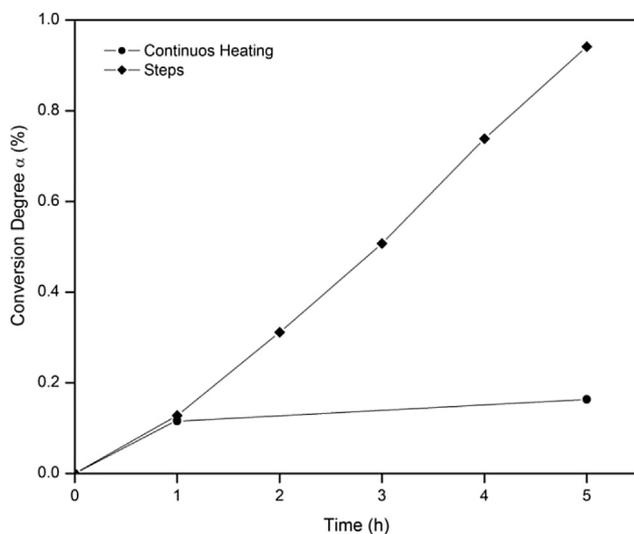
Fig. 8 – Comparison of conversion degrees obtained in a continuous heating test (up to 5 h) and interrupted heating tests (5 steps of 1 h each) at 823 K.

concluded that the extraction of the hydrogen produced from the reactor is clearly beneficial for shifting the thermochemical reactions to the proper side that enhances the hydrogen production. Similar experiments at 923 K and 1223 K showed that the extraction of hydrogen from the reactor had a smaller influence for enhancing the hydrogen production.

Interrupted heating tests were also done at 1223 K at heating cycles of 24 h each. After 5 successive heating steps, a conversion degree of 30% was achieved instead of 15% obtained during a continuous heating test at the same temperature.

Experimental results at low pressure have shown clearly that an increment of the reaction temperature is not expected to affect strongly the amount of hydrogen produced by this thermochemical cycle. In order to explore for more favorable
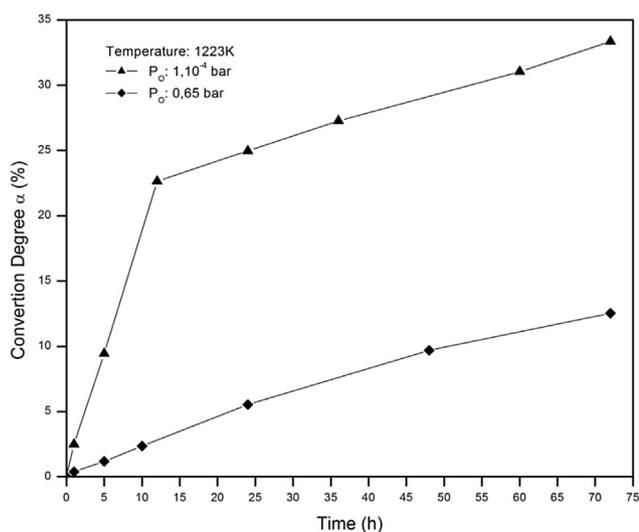
Fig. 9 – Conversion degree as a function of the system pressure at 1223 K.

conditions for the hydrogen production through this cycle, the pressure of experimental system was increased by adding different amounts of argon gas into the reactor before heating. When the reactor temperature was increased during heating, the inner reactor pressure increased too, in a magnitude that depends on the amount of argon gas added at room temperature.

Two experiments were carried out at 1223 K with different amounts of argon gas introduced into the reactor before heating. When the reactor reached the reaction temperature, the system pressure was estimated to be 2.67 bar (P_o = 0.65 bar). As can be seen in Fig. 9, these new experimental conditions appear to be very beneficial for the hydrogen production since the conversion degree after 10 h of continuous heating was remarkably increased from 2.5% at low pressure to 24% at 2.67 bar.

Reaction kinetics and proposal of a modified Fe-Cl cycle

Considering that chemical species detected by analysis were: Fe_3O_4, HCl, Cl_2, iron chloride (II) and (III), condensed water and molecular hydrogen, it is possible to confirm that the Mark-15 Fe-Cl cycle proceeds through the reactions given by Equations (1)–(4), producing the global water-splitting reaction indicated by Equation (5).

It is well-known that reactions (1) and (2) are very fast in the range of temperatures studied [27], while the reaction (3) is slow enough to be considered as the rate determining step for the hydrogen production through this thermochemical cycle [28].

This reaction sequence confirmed by experimental results is indicating that the kinetics of the Mark-15 Fe-Cl cycle has an important dependence with the system pressure. In effect, if the rate determining step of the overall process is the reaction (3), then reactions (1) and (2) are in equilibrium and reaction (2) has a lower amount of gaseous moles on the right side than on the left side, so that an increase in the reaction pressure shifts the reaction (2) towards the formation of products, explaining the increment of the conversion degree observed at pressures above atmospheric.

In order to increase the overall energy efficiency of the Mark-15 cycle, a modified version of the cycle is proposed by reducing the two high-temperature reactions given by Equations (1) And (4) from 1198 K to 923 in order to avoid the phase change of $FeCl_2$ that melts at 950 K, while an additional benefit is expected due to the reduction of the separation work that is proportional to the reaction temperature. The proposal is based on a former experimental evidence which demonstrated that the reverse Deacon reaction and the hydrolysis of $FeCl_2$ can run at lower temperatures than those originally proposed (Ref. [20]), but it was also confirmed by our experiments in the case of reaction (1), since the $FeCl_2$ was observed to be deposited between zones I and II of reactor, where the temperature ranges between 923 K and 573 K.

For the calculation of the limiting energy efficiency of the modified Mark-15 cycle, the global cycle was decomposed into elementary reaction steps for thermal enthalpy balance as shown in Fig. 10.
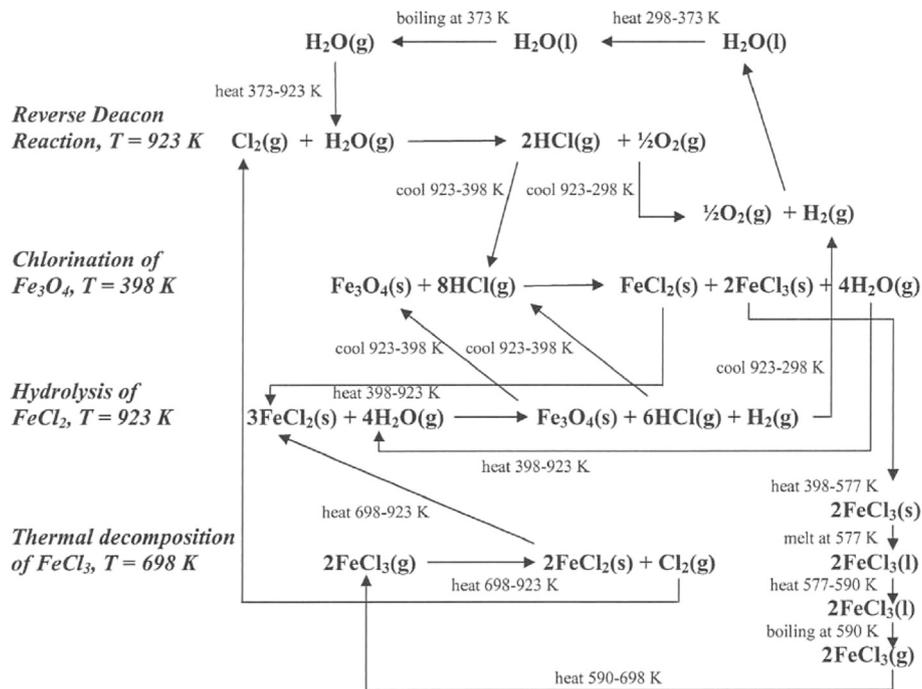
Fig. 10 – Decomposition of the modified Mark-15 Fe-Cl cycle into elementary steps for thermal enthalpy balance analysis.

Calculation results of enthalpy balance are presented in Table 8. As in the former analysis, T_{in} and T_{out} define the starting and finishing temperatures of each individual step while ΔH y ΔG represent the changes of enthalpy and standard Gibbs free energy, respectively. The first four steps comprise the thermochemical reactions given by Equations (1)–(4), while the remaining sixteen steps involve the heating and cooling processes and the phase changes of H_2O and $FeCl_3$.

Results of heat and work input calculations for the modified Mark-15 cycle are presented in Table 9. In comparison with the original Mark-15 Fe-Cl cycle, it is seen that heat and work requirements for the modified cycle are reduced and it is mainly due to a decrease in the magnitude of separation and chemical potential work components, as a consequence of lowering the two high-temperature thermochemical reactions.

Compound	Reaction	Type	Moles	Tin [K]	Tout [K]	ΔH [kJ]	ΔG [kJ]
Fe₃O₄(s)	Fe₃O₄ + 8HCl → FeCl₂ + 2FeCl₃ + 4H₂O	Reaction	1	398	398	−244.5	−58.9
FeCl₂(s)	3FeCl₂ + 4H₂O → Fe₃O₄ + 6HCl + H₂	Reaction	3	923	923	337.5	51.2
FeCl₃(g)	2FeCl₃ → 2FeCl₂ + Cl₂	Reaction	2	698	698	−160.5	−23.9
Cl₂(g)	Cl₂ + H₂O → 2HCl + ½O₂	Reaction	1	923	923	58.9	−3.8
H₂O(l)	Sensible	Heat 298-373 K	1	298	373	5.7	
H₂O(l)→H₂O(g)	Latent	Boiling	1	373	373	40.9	
H₂O(g)	Sensible	Heat 373-398 K	1	373	398	0.9	
H₂O(g)	Sensible	Heat 398-923 K	5	398	923	94.4	
Cl₂(g)	Sensible	Heat 698-923 K	1	698	923	5.4	
FeCl₃(s)	Sensible	Heat 398-577 K	2	398	577	47.3	
FeCl₃(s)→FeCl₃(l)	Latent	Melting	2	577	577	112.9	
FeCl₃(l)	Sensible	Heat 577-590 K	2	577	590	3.4	
FeCl₃(l)→FeCl₃(g)	Latent	Boiling	2	590	590	154.0	
FeCl₃(g)	Sensible	Heat 590-698 K	2	590	698	28.1	
FeCl₂(s)	Sensible	Heat 398-698 K	1	398	698	27.0	
FeCl₂(s)	Sensible	Heat 698-923 K	3	698	923	60.8	
Fe₃O₄(s)	Sensible	Cool 923-398 K	1	923	398	−75.1	
HCl(g)	Sensible	Cool 923-398 K	8	923	398	−121.8	
O₂(g)	Sensible	Cool 923-298 K	0.5	923	298	−10.0	
H₂(g)	Sensible	Cool 923-298 K	1	923	298	−18.1	
					TOTAL	347.2	

Table 8 – Enthalpy balance for the modified Mark-15 Fe–Cl thermochemical cycle.

Table 9 — Heat and work inputs estimated for the modified Mark-15 Fe–Cl cycle.

	Energy [kJ/mol H_2]	Heat equivalent[a] [kJ/mol H_2]
Total heat-in	347.2	347.2
Heat rejected	206.2	206.2
Separation work	53.6	107.2
Chemical potential work	51.2	102.4
Sum of heat and work inputs		763.0

[a] A 50% conversion factor is assumed which is based on the heat available from a high-temperature gas cooled nuclear reactor.

Finally, the limiting energy efficiencies of the modified Mark-15 cycle can be estimated as follows:

- Lower heating value (LHV) $= \frac{241.8}{763.0} \times 100 = 32\%$
- Higher heating value (HHV) $= \frac{285.8}{763.0} \times 100 = 37\%$

It can be appreciated that a decrease of the two high-temperature reactions from 1198 K to 923 K seems to be beneficial for increasing the overall energy efficiency of the Mark-15 Fe-Cl cycle due to a significant reduction of separation and chemical potential works.

Conclusions

In this paper, it was demonstrated that the Mark-15 Fe-Cl thermochemical cycle may be produced in a batch reactor under different experimental conditions of reaction temperatures, pressures, and holding times. The theoretical and experimental study carried out at laboratory scale was addressed to elucidate the reaction pathway and the kinetics of this thermochemical cycle in order to improve its overall performance in terms of both energy and hydrogen yield, as a previous step for a further scaling up of experimental facilities.

A thermodynamic analysis was firstly done in order to estimate the theoretical limiting energy efficiency of the cycle and the effect of changing the ratio between the reagents H_2O and $FeCl_2$ on the conversion degrees. Following, proof-of-concept experiments were performed at atmospheric pressure and different temperatures and reaction times. Additional tests were carried out in successive heating steps after extracting the gaseous products from the reactor at the end of each heating step. The effect of increasing the system pressure on the hydrogen yield was also studied.

On the basis of experimental results and the characterization of solid and gaseous reaction products, it was possible to confirm that the reaction pathway for hydrogen production is expected to happen according to that originally proposed. The rate determining step of the overall process was identified and the beneficial effect on the hydrogen yield of increasing the system pressure could be explained.

Finally, a modified version of the Mark-15 Fe-Cl cycle is proposed for increasing its overall energy efficiency. The proposal consists of reducing the two high-temperature reactions given by Equations (1) And (4) from 1198 K to 923 in order to avoid the phase change of $FeCl_2$ that melts at 950 K. It is based on a former experimental evidence which demonstrated that the reverse Deacon reaction and the hydrolysis of

$FeCl_2$ can run at lower temperatures than those originally proposed (Ref. [20]), but it was also confirmed by our experiments in the case of reaction (1), since the $FeCl_2$ was observed to be deposited between zones I and II of reactor, where the temperature ranges between 923 K and 573 K.

Comparative calculations of enthalpy balance and external heat and work requirements for the original and modified cycles showed that the limiting energy efficiency can be theoretically increased from the range 24-28% to 32-37% and this significant increment appears to be attractive for further investigations on the Mark-15 Fe-Cl cycle.

REFERENCES

[1] The Hydrogen Economy: Opportunities, costs, barriers and R&D needs. Committee on Alternatives and Strategies for Future Hydrogen Production and Use. National Research Council, National Academy of Engineering; 2004.

[2] Energy technology perspectives 2008-Scenarios and strategies to 2050. International Energy Agency; 2008.

[3] Annual progress report, U.S. DOE hydrogen program. 2009.

[4] Sato S. Thermochemical hydrogen production. In: Ohta T, editor. Solar-hydrogen energy systems. Pergamon Press; 1979. p. 81–114.

[5] Funk JE, Reinstrom RM. Energy requirements in the production of hydrogen from water. IEEC Process Des Dev 1966;5:336–42.

[6] Funk JE. Thermochemical hydrogen production: past and present. Int J Hydrogen Energy 2001;26:185–90.

[7] Russell Jr. JL et al. Water splitting–A progress report. Proc. 1st World Hydrogen Energy Conference, Miami Beach, March 1976, 1, p.1A105-1A124.

[8] Yamawaki M, et al. Application of nuclear energy for environmentally friendly hydrogen generation. Int J Hydrogen Energy 2007;32:2719–25.

[9] Lewis MA, Taylor A. High temperature thermochemical processes. DOE Hydrogen Program, Annual Progress Report, Washington DC 2006:182–5.

[10] Wang ZL, et al. Comparison of different copper-chlorine thermochemical cycles for hydrogen production. Int J Hydrogen Energy 2009;34:3267–76.

[11] Lemont F. Promising optimization of the $CeO_2/CeCl_3$ cycle by reductive dissolution of cerium(IV) oxide. Int J Hydrogen Energy 2008;33:7355–60.

[12] Cremer H, et al. Status report on thermochemical iron/chlorine cycles: a chemical engineering analysis of one process. Int J Hydrogen Energy 1980;5:231–52.

[13] Knoche KF, et al. Thermochemical production of hydrogen by a vanadium/chlorine cycle. II: experimental investigation of the individual reactions. Int J Hydrogen Energy 1984;9:473–82.

[14] Van Velzen D, Langenkamp H. Development studies on thermochemical cycles for hydrogen production. Int J Hydrogen Energy 1977;2:107–21.

[15] Knoche KF, Cremer H, Steinborn G. A thermochemical process for hydrogen production. Int J Hydrogen Energy 1976;1:23–32.

[16] Knoche KF, et al. Feasibility studies of chemical reactions for thermochemical water splitting cycles of the iron-chlorine, iron-sulfur and manganese-sulfur families. Int J Hydrogen Energy 1977;2:269–89.

[17] Yalçin S. A review of nuclear hydrogen production. Int J Hydrogen Energy 1989;14:551–61.

[18] Beghi GE. A decade of research on thermochemical hydrogen at the joint research centre, Ispra. Int J Hydrogen Energy 1986;11:761–71.

[19] Lewis MA, Masin JG. The evaluation of alternative thermochemical cycles-Part II: the down-selection process. Int J Hydrogen Energy 2009;34:4125–35.

[20] Gahimer J, Mazumder M, Pangborn J. Experimental demonstration of an iron chloride thermochemical cycle for hydrogen production. In: Eleventh intersociety energy conversion engineering conference, Sahara Tahoe hotel, state line, USA; 1976. p. 933–9.

[21] HSC software: Outukumpu HSC chemistry for windows version 6.12. Pori, Finland: Outukumpu Research Oy; 2006.

[22] Lewis MA, Masin JG, ÓHare PA. Evaluation of alternative thermochemical cycles. Part I: the methodology. Int J Hydrogen Energy 2009;34:4115–24.

[23] Linnhoff B, Polley GT. General process improvements through pinch technology. Chem Eng Prog June 1988.

[24] Andress RJ, et al. A systematic methodology for the evaluation of alternative thermochemical cycles for hydrogen production. Int J Hydrogen Energy 2009;34:4146–54.

[25] Carty RH, Mazumder MM, Schreider JD, Pangborn JB. Thermochemical hydrogen production, vols. 1–4. Gas Research Institute for the Institute of Gas Technology; 1981. GRI-80/0023.

[26] Lide DR. Properties of the elements and inorganic compounds, in CRC handbook of chemistry and physics. Internet Version 2005. Boca Raton, FL: CRC Press; 2005., http://www.hbcpnetbase.com.

[27] Bertoti I, Pap I, Székely T, Babievskaya I, Bottyán L, et al. TG studies on the reactions of hematite, magnetite and wustite with CL_4. Thermochim Acta 1985;85:87–90.

[28] Ma K, Zhu Z, Yan C. Separation of cobalt from iron by chloride hydrolysis at elevated temperatures. J Mater Sci Technol 1997;13:421–4.